MECHANICAL EFFECTS OF BOTULINUM TOXIN TREATMENT ON ISOLATED MUSCLE: ASSESMENT OF THEORETICAL PARALYZATION PATTERNS VIA FINITE ELEMENT MODELING

by

Ahu Nur Türkoğlu

B.Sc., Physics, Boğaziçi University, 2008

Submitted to the Institute of Biomedical Engineering
in partial fulfillment of the requirements
for the degree of
Master of Science
in
Biomedical Science

Boğaziçi University
2010

MECHANICAL EFFECTS OF BOTULINUM TOXIN TREATMENT ON ISOLATED MUSCLE: ASSESMENT OF THEORETICAL PARALYZATION PATTERNS VIA FINITE ELEMENT MODELING

APPROVED BY:

Assoc. Prof. Dr. Can A. Yücesoy .....
(Thesis Advisor)

Prof. Dr. Mehmed Özkan .....

Assist. Prof. Dr. Ekin Akalan .....

DATE OF APPROVAL: 06 September 2010

ACKNOWLEDGMENTS

First and foremost, I would like to thank my thesis advisor, Assoc. Prof. Dr. Can A. Yücesoy, for his guidance throughout my study. Also, I would like to thank my thesis examining committee Prof. Dr. Mehmed Özkan and Assist. Prof. Dr. Ekin Akalan for their valuable comments and recommendations.

I would like to thank my friends in Biomechanics Laboratory Filiz Ateş, Emre Arıkan, Oya Aytürk, Zeynep Susam, Selen Ersoy and Turgay Ertugay for their helpfulness, support, advice and valuable time.

Finally, I would like to express my gratitude to my mother, for her love, encouragement, patience and support that made everything possible. I dedicate this dissertation to my mother.

ABSTRACT

MECHANICAL EFFECTS OF BOTULINUM TOXIN TREATMENT ON ISOLATED MUSCLE: ASSESMENT OF THEORETICAL PARALYZATION PATTERNS VIA FINITE ELEMENT MODELING

The specific goal of the present study was to take an initial step in explaining the effects of Botulinum toxin treatment used for muscle pathologies such as spasticity on muscle mechanics via myofascial force transmission, which we believe is a major determinant. For this purpose an isolated EDL muscle model generated using the finite element method was used. In order to determine the effect of paralyzation location three cases were studied: Proximal half passive, middle half passive and distal half passive. Strain and stress distributions and length-force relationships of these cases were compared. Length-force relationship showed about 50% foce drop at optimum length for all three cases whereas at low lengths, distal half paralyzed case showed up to 15% more force reduction than other two cases. This result may be significant for spastic muscles since they are reported to operate at low muscle lengths. Also range of active force exertion decreased up to 23%. A significant result obtained from strain distributions is that the mechanically operational parts, i.e. parts that are not affected by Botulinum toxin showed less shortening compared to their counterparts in the non-paralyzed muscle. It is evident that this effect arises from the interaction between mechanically operational and paralyzed muscle portions. Such effect is a clear indication of intramuscular myofascial force transmission pathways.

Keywords: Botulinum toxin, Myofascial force transmission, Isolated muscle, Finite element modeling, Sarcomere length distribution.

ÖZET

BOTULİNUM TOKSİN TEDAVİSİNİN İZOLE KAS ÜZERİNDEKİ ETKİLERİ: TEORİK PARALİZASYON ŞEKİLLERİNİN SONLU ELEMANLAR ANALİZİ İLE DEĞERLENDİRİLMESİ

Çalışmanın ana hedefi spastisite gibi hastalıkların tedavisinde kullanılan Botulinum toksinin kas üzerindeki mekanik etkilerini ana bir belirleyici olduğunu düşündüğümüz miyobağdokusal kuvvet iletimi ışığında incelenmesidir. Bunun için sonlu elemanlar yöntemi ile oluşturulmuş izole EDL kası modeli kullanılmıştır. Paralizasyon konumunun etkilerinin incelenmesi için üç durum oluşturulmuştur: proksimal yarı paralize, orta yarı paralize ve distal yarı paralize. Bu durumların uzunluk-kuvvet ilişkileri ve gerilim ve gerinim dağılımları Botulinum toksin uygulanmamış kas modeli ile karşılaştırılmıştır. Optimum boylarda her üç durum için de % 50 civarında kuvvet düşüşü bulunurken, kısa boylarda durumlar arası fark % 15 civarına çıkabilmektedir. Spastik kasların kısa boylarda aktivite göstermesi bu sonucu önemli kılmaktadır. Uzunluk-kuvvet ilişkisinin ortaya çıkardığı bir diğer önemli sonuç ise toxin uygulanan durumlarda aktif kuvvet aralığının % 23'lere kadar düşebildiğidir. Gerinim dağılımlarının ortaya çıkardığı önemli bir sonuç ise toksinden etkilenmeyen bölgelerin, toksin uygulanmamış durumdaki eşlerine göre daha az kısalmalalarıdır. Bu etkiye toksinden etkilenmiş bölgeler ve mekanik olarak işlevsel bölgeler arası etkileşimin neden olduğu aşikardır. Bu tür bir etkileşimse intramüsküler miyobağdokusal kuvvet iletiminin göstergesidir.

Anahtar Sözcükler: miyobağdokusal kuvvet iletimi, izole kas, Botulinum toksin, sonlu elemanlar modellemesi.

TABLE OF CONTENTS

LIST OF FIGURES

LIST OF TABLES

LIST OF ABBREVIATIONS

MFT	Myofascial Force Transmission
LFMM	Linked Fiber-Matrix Mesh
EDL	Extensor Digitorum Longus muscle
EHL	Extensor Hallucis Longus muscle
PHP	Proximal half paralyzed
MHP	Middle half paralyzed
DHP	Distal half paralyzed
CV	Coefficient of variation

1. INTRODUCTION

1.1 Skeletal Muscle

1.1.1 Structure

Muscular tissue is composed of cells varying from 100 μm to 500 μm in diameter and 3 to 30 cm at length, that contract when stimulated. A muscle cell is essentially a device for converting the chemical energy of ATP into the mechanical energy of contraction. There are three types of muscle tissue: skeletal, cardiac, and smooth. However, only skeletal muscle is responsible for joint movement. Skeletal muscle is typically attached to one or more bones via its tendons (Figure 1.1) [1]. The very regular arrangement of the myofibrils and their subunits in the individual muscle cells can be seen in the optical microscope as regular light and dark bands, which have given skeletal muscle the name striated muscle [2].

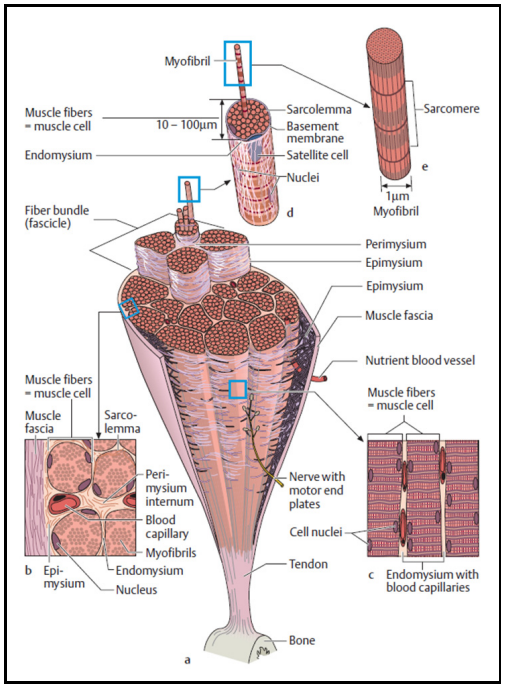

Figure 1.1 Structure of a skeletal muscle (a) Cross-section of a skeletal muscle (b) Magnified section from a (cross-section) (c) Magnified section from a (longitudinal section) (d) Structure of a muscle fiber (muscle cell) (e) Structure of a myofibril [1]

In skeletal muscle, muscular fibers and connective tissue are closely interlinked. A strong connective tissue sheath consisting of dense collagen connective tissue (muscle fascia) surrounds the muscle, contains it, and allows it to slide through its related structures. Each muscle is composed of individual bundles of fibers (fascicles) and are connected by areolar tissue (epimysium). Blood vessels and nerves are contained in the epimysium and access the internal part of the muscle. The individual fiber bundles are also composed of hundreds of muscle fibers that are enveloped in another connective tissue sheath (endomysium) and are also connected with each other by areolar tissue (perimysium). Each muscle cell is a long tube of cytoplasm surrounded by a cell membrane (sarcolemma) and possesses several hundred nuclei along its sides. They usually run the whole length of a muscle and merge at both ends into connective tissue tendons that connect the muscle to bone. These different levels of connective tissues are continuous up to the tendons [3].

It should be noted that collagen is not excitable or contractile, but it is extensible and elastic. It can stretch under tension and recoil when released. Because of this elasticity and because the connective tissue components are connected to each other in a linear series, the connective tissues are called the series-elastic components of a muscle [2]. Their elasticity helps to return muscles to their resting lengths when contraction ceases. Elastic recoil of the tendons adds significantly to the power output and efficiency of the muscles [3].

1.1.2 Muscle Fiber

Muscle fibers are multinucleated, with the nuclei located just under the plasma membrane. Most of the cell is occupied by myofibrils. Within each myofibril there are dense Z lines with a sarcomere in between. Hundreds of these sarcomeres (or muscle functional unit) form a muscle fiber. Each sarcomere has thick and thin filaments (Figure 1.2). The thick filaments are made of myosin and occupy the center of each sarcomere. Thin filaments are made of actin and anchor to the Z line [1].

Muscle contracts by forming cross-bridges between thin and thick filaments [3]. The sliding filament model of muscle contraction has thin filaments on each side of the sarcomere sliding past each other. Myosin filaments have heads that bend toward the actin filaments [2].

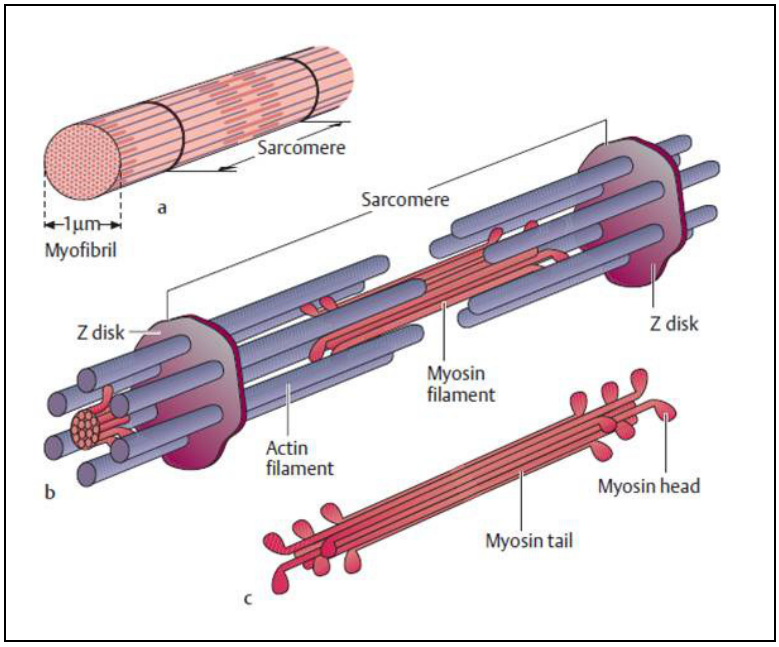

Figure 1.2 Schematic representation of the structure of a sarcomere (a) Myofibril (b) Arrangement of actin and myosin filaments in the sarcomere (c) Structure of a myosin filament[1]

Myosin heads attach to binding sites on the actin filaments. The myosin heads pull toward the center of the sarcomere, detach and then reattach to the nearest active site of the actin filament. Each cycle of attachment, pulling, and detachment generates force. Hundreds of such cycles occur each second during muscle contraction. Energy for this comes from ATP. ATP binds to the cross bridges between myosin heads and actin filaments. The release of energy powers the pulling of the myosin head. Calcium ions are required for each cycle of myosin-actin interaction. Calcium is released into the sarcomere when a muscle is stimulated to contract. This calcium uncovers the actin binding sites. When the muscle no longer needs to contract, the calcium ions are pumped from the sarcomere and back into storage [2, 3].

1.2 Force Transmission Pathways

A skeletal muscle is divided into variously shaped muscle belly and the usually thinner tendons. The tendons are attached to structures in the skeleton or connective tissue of the locomotor system (fasciae, interosseous membrane) and transmit the muscle force directly or indirectly to parts of the skeleton [4]. Force generated within sarcomeres is transmitted to sarcomeres in series and therefore delivered to the tendons and bone tissue via myotendinous junctions [4]. The importance of myotendinous force transmission is widely accepted and such force transmission has been studied extensively [5, 6]. However, accepting myotendinous pathway as the sole force transmission pathway recently shown to be a mechanically incomplete concept [7]. The role of connective tissue has proved itself to be functional in force transmission and this new kind pathway is referred to as *myofascial force transmission* [8, 4].

1.2.1 Myotendinous Force Transmission

The myotendinous force transmission is the primary pathway for the transmission of force generated within the muscle belly. Muscular connective tissues i.e. endomysium, perimysium and epimysium, are continuous structures and combine to form the aponeurosis and the tendon of the muscle. At the muscle endings the sarcolemma of the muscle fibers greatly decrease in diameter and fold longtiduonally. At these sites collagen fibers are present and combine with the collagen matrix of the muscle. The force is assumed to be transmitted by these structures [4]. Experimental studies (e.g., [9, 5]) as well as biomechanical modelling studies (e.g., [10]) indicate that shearing of the basal lamina is the principal mechanism involved in transmission of force from the myofibril to the tendinous collagen.

Accepting the myotendinous force transmission as the exclusive transmission pathway would require equal forces to be exerted at both ends of the muscle. This consideration has been nurtured until recently due to experimental work involving whole muscle isolated except for its blood supply [11], isolated small muscle fascicles

[12] and single muscle fibres.

1.2.2 Myofascial Force Transmission

Activatable muscle fibers and passive connective tissue structures are connected mechanically not only at the fiber ends where these structures are connected to tendinous tissues but also along the full peripheral surface of muscle fibers. Upon this knowledge in addition to myotendinous force transmission, a second pathway has been shown to exist, that uses the muscle's cytoskeletal lattice and trans-sarcolemmal molecules as well as basal lamina connecting molecules to transmit force onto connective tissue. This second mechanism of force transmission, i.e. myofascial force transmission, was shown to be important in experiments [13]designed specifically: Street (1983) studied mechanical connections between myofibrillar components and sarcolemma. Upon activating a partially isolated fiber, tension was recorded from surrounding tissue at the non-isolated part of the fiber. Hence Street concluded that both active and resting tension were transmitted laterally [12].

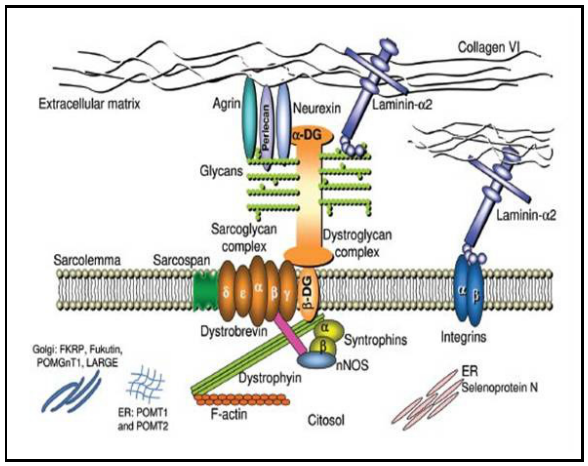

Figure 1.3 Schematic representation of organization of transsarcolemmal connections in a muscle fiber

A muscle in vivo would interact with its surroundings, hence differ the mechanical equilibrium of the entire limb. The role played by the continuous system of collagen matrix in force transmission has been made evident at different levels. The pathways of myofascial force transmission are therefore classified in two groups:

(1)*Intramuscular myofascial force transmission*:The force generated by the sarcomeres are transmitted to the transsarcolemmal proteins via the cytoskeleton of the fiber (Figure 1.3). Such force transmission continues up to the endomysium.(Figure 1.1). The continuous nature of the collagen matrix surrounding the fibers has been explained previously in this text. This hierargical continuation from endomysium to epimysium and perimysium ensures the continuity of the force transmission, itself. Such transmission of force occuring within the muscle is referred to as intramuscular myofascial force transmission and is the main interest in this study.

A previous study on tenatomy on Extensor digitorum longus (EDL) muscle by Huijing et al. [14] showed that EDL force production remained at high levels after acute tenotomy and muscle length-force curves did not change significantly. Therefore, it was concluded that force transmission occurred between heads of the EDL myofascially. Moreover, alterations on intramuscular connections such as separation of the interface between heads leading to substantial force drop supported this conclusion.

(2)*Epimuscular myofascial force transmission*:The force produced by a muscle can be exerted also onto synergist muscle groups or other structures such as compertmantel bounderies.

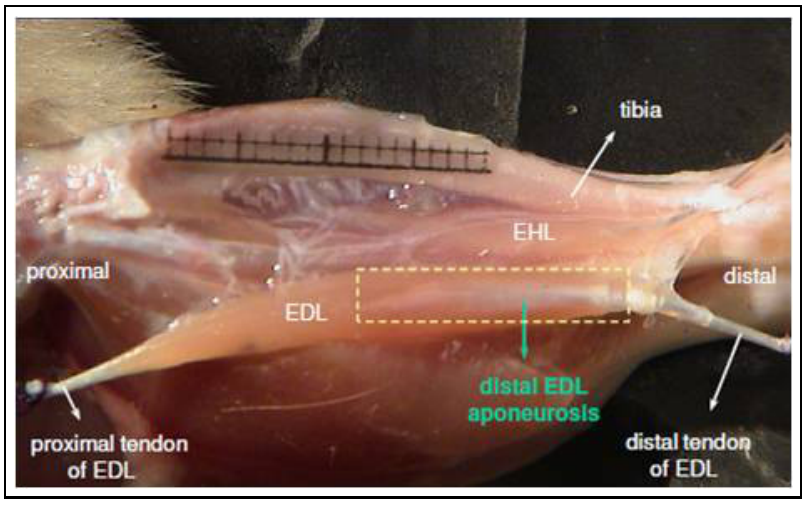

Figure 1.4 EDL muscle with its connective tissue

The connection between muscles' epimysium and synergist groups' epymisia is

capable of force transmission [15] and such transmission is referred to as intermuscular myofascial force transmission [16]. Several studies report direct evidence on *intermuscular myofascial force transmission.* A study on epimuscular connections between EDL and EHL, by Yucesoy et al. [15] reports the myofascial pathways between these two muscles are sufficiently stiff to transmit force even after small changes in relative position of a muscle with respect to its neighboring muscular and nonmuscular tissues.

In this study also the non-muscular tissues surrounding the muscle were reported to be effective in force transmission. The transmission of force from the extracellular matrix onto elements such as fascie, intermuscular septa, interrosseal membranes, epitendinous tissues, neurovascular tracts and bones is referred to as *extramuscular myofascial force transmission* [17].

Such force transmission to the outside of the muscle has been shown to have major effects on muscle mechanics;(1) substantial proximo-distal force differences [16](2) altered length-force characteristics [15, 16, 18] and (3) sarcomere length heterogeneity [16].

1.3 Botulinum Toxin Treatment

Spasticity is a velocity-dependent increase in muscle tone with exaggerated tendon jerks but the term is often used to refer to the upper motor neuron syndrome [19]. Disability occuring due to spasticity is often very difficult to treat. Medications such as baclofen, benzodiazepines and tizanidine, and physical therapy are used clinically. Local treatments to weaken specific muscles are also used widely. Botulinum Toxin-A is the most commonly used agent for this purpose. Botulinum toxin temporarily reduces excessive muscular contraction in the target muscle. The main aim of this treatment is to improve patient function by increasing joint range of motion. It was shown to be most effective in patients with localised dynamic muscle shortening [19].

Botulinum toxin may be successfully used for the treatment of particular muscle

groups, as long as a clear functional goal is identified. Early treatment is preferable for maximum response and prolonged effects, and because of the potential to reduce contractures and delay surgery. In older children, responses are generally less pronounced, shorter-lived and increasingly inhibited by the presence of fixed contractures. The optimal timing for Botulinum Toxin-A treatment is reported to be between 1 and 5 years of age, during the period of dynamic motor development, where there is the greatest chance of modifying the course of the disease [20].

Botulinum Toxin-A may also be successfully used for treating other muscular disorders such as muscular hyperactivity in childhood resulting from a number of other causes, particularly traumatic brain injury, as well as hereditary spastic paraplegia and spina bifida [21].

1.4 Goal of the Study

The studies on Botulinum toxin treatment have the goal of increasing the paralyzed muscle portion at their center. The idea is maximal force reduction for increased active range of motion of the muscle. In the literature, studies on locating the motor-end plates [22], injection location and dose [23] are abundant. These studies lead to empirical data on how to increase force reduction because none explains or considers mechanical effects associated.

The specific goal of the present study is to take an initial step in explaining the effects of Botulinum toxin treatment on muscle mechanics via myofascial force transmission, which we believe to be a major determinant. By using finite element analysis, isolated rat EDL muscle is modeled and variations in paralyzed area location are investigated. For this purpose, previously developed "linked fiber-matrix mesh model" is advanced by adapting a finer mesh in the same geometry. The effects of intramuscular connections are studied.

2. METHODS

2.1 Description of the "Linked Fiber-Matrix Mesh model"

Using the linked fiber-matrix mesh model (LFMM model [16]) created in accordance with experimental data on muscle properties, skeletal muscle is considered explicitly as two separate domains: (1) the intracellular domain and (2) extracellular matrix domain. The transsarcolemmal attachments are considered as elastic links between the two domains. Two self-programmed elements were developed and were introduced as user-defined elements into the finite element program ANSYS 9.0: (1) extracellular matrix element represents the collagen reinforced extracellular matrix, which includes the basal lamina and connective tissue components such as endomysium, perimysium and epimysium. (2) myofiber element models the muscle fibers. Within the biological context, each combined muscle element represents a segment of a bundle of muscle fibers with identical material properties, its connective tissues and the links between them. This is realized as a linked system of extracellular matrix and myofiber elements (for a schematic 2D-representation of an arrangement of these muscle elements see [16]). A whole fascicle is constructed by putting three muscle elements in series.

In the LFMM model, the extracellular matrix domain is represented by a mesh of extracellular matrix elements (matrix mesh). In the same space, a separate mesh of myofiber elements is built to represent the intracellular domain (fiber mesh). The two meshes are rigidly connected to single layers of elements modeling proximal and distal aponeuroses: a node representing myotendinous connection sites is the common node of all three (extracellular matrix, myofiber and aponeurosis) elements. In contrast, at the intermediate nodes, fiber and matrix meshes are linked elastically to represent the transmembranous attachments of the cytoskeleton and extracellular matrix. For these links (the model includes a total of 28 of them: 14 in each of the upper and lower model surfaces) the standard element, COMBIN39 is used from the element library of

ANSYS 9.0. This is a 2-node spring element, which is set to be uni-axial and have linear high stiffness characteristics representing non-pathological connections between the muscle fibers and the extracellular matrix (for an analysis of the effects of stiff or compliant links see [16]). Note that at the initial muscle length (28.7 mm) and in passive condition, these links have a length equaling zero.

Extracellular matrix and myofiber elements have eight nodes, linear interpolation functions and a large deformation analysis formulation are applied. A 3D local coordinate system representing the fiber, cross-fiber (normal to the fiber direction), and thickness directions is used. The stress formulation $\underline{S}$ based on Second Piola-Kirchoff definition constitutes the derivative of the strain energy density function, W; with respect to the Green-Lagrange strain tensor, $\underline{L}^G$.

$$\underline{S} = \frac{dW}{d\underline{L}^G} \tag{2.1}$$

2.1.1 Extracellular Matrix Element

The strain energy density function mechanically characterizing the extracellular matrix includes two parts:

$$W = W_1 + W_2 \tag{2.2}$$

The first part represents the non-linear and anisotropic material properties [24]:

$$W_1 = k.(e^{a_{ij}.z_{ij}} - a_{ij}.\epsilon_{ij}) \; for \; \epsilon_{ij} > 0 \; or, \tag{2.3}$$

$$W_1 = -W_{ij}(|\epsilon_{ij}|) \; for \; \epsilon_{ij} < 0 \; and \; i \neq j \tag{2.4}$$

where ϵ_{ij} are the Green-Lagrange strains in the local coordinates. The indices $i = 1, ..., 3$ and $j = 1, ..., 3$ represent the local cross-fiber, fiber and thickness directions, respectively. a_{ij} and k are constants (Table 2.1). The resulting stress-strain curves are shown in Figure 2.1. The second part includes a penalty function to account for the

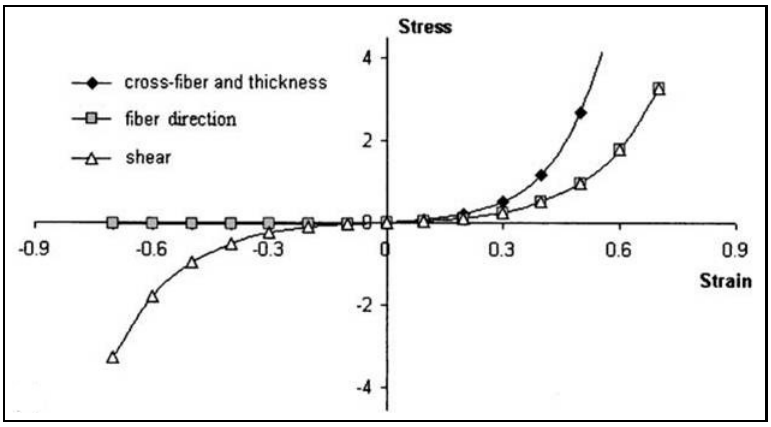

Figure 2.1 Passive non-linear and anisotropic material properties of the extracellular matrix element in the local coordinates

constancy of muscle volume

$$W_2 = S_s.(I_3 - 1)^2 + S_f.(I_{avg}^3 - 1) \tag{2.5}$$

where I_3 is the third invariant (determinant) of the Right Cauchy-Green strain tensor and is a measure for the local volume for each Gaussian point. To conserve the local volumes (i.e. I_3 equals unity), the element is considered as incompressible solid. In contrast, if the weighted mean of all I_3s per element (I_{avg}^3) is kept as unity, the element is considered to be a fluid. Using the penalty parameters ls (for the solid volume) and lf (for the fluid volume) (Table 1), the emphasis given for each part can be manipulated.

2.1.2 Myofiber Element

Maximally activated muscle is studied and within the muscle fibers, sarcomeres are assumed to have identical material properties. The force-velocity characteristics are not considered due to the isometric nature of the present work. The total stress for the intracellular domain (σ_{22_f}) is a Cauchy stress acting only in the local fiber direction and is the sum of the active stress of the contractile elements ($\sigma_{22_{contr}}$) and the stress due to intracellular passive tension ($\sigma_{22_{icp}}$). To define the active length-force characteristics, an exponential function (Figure 2.2) was fit to the experimental data of small rat GM fiber bundles [25]. This function is scaled such that at optimum length,

the fiber direction strain (ϵ_{22}) is zero and the maximal stress value is unity,

$$\sigma_{22_{contr}}(\epsilon_{22}) = b_3 e^{b_2 \epsilon_{22}^3} \; for \; \epsilon_{ij} > 0 \; or, \tag{2.6}$$

$$\sigma_{22_{contr}}(\epsilon_{22}) = b_3 e^{b_1 \epsilon_{22}^4} \; for \; \epsilon_{ij} < 0 \tag{2.7}$$

where b_1, b_2 and b_3 are constants

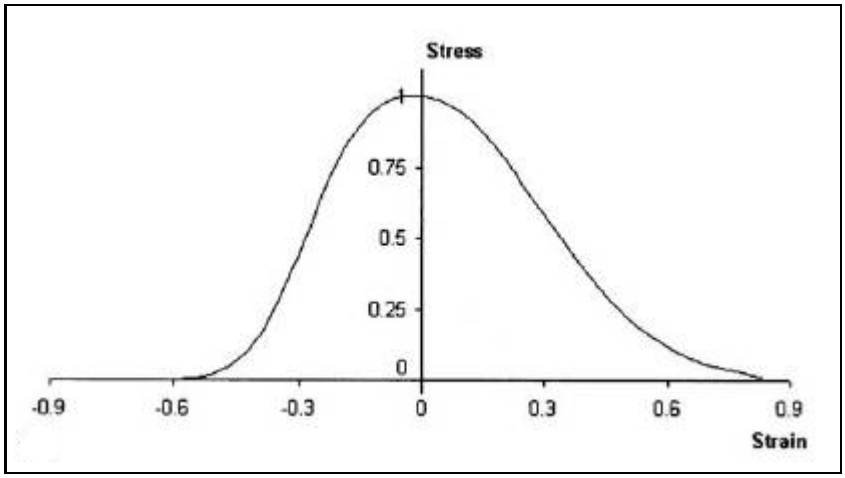

Figure 2.2 Active stress strain properties of the myofiber element representing the contractile apparatus, which is only valid for the local fiber direction

The source of intracellular passive tension is the intrasarcomeric cytoskeleton [26], which is composed of several proteins. In this work, titin is considered to play the dominant role. Experimental tension-sarcomere length data [26] for a single rabbit skeletal muscle fiber was fitted using a parabolic function (Figure 2.3) and scaled to make it compatible to the stress-strain characteristics of the contractile part.

$$\sigma_{22_{contr}}(\epsilon_{22}) = t_1 \epsilon_{22}^2 + t_2 \epsilon_{22} + t_3 \; for \; \epsilon_{22} > 0 \; and \tag{2.8}$$

$$\sigma_{22_{contr}}(\epsilon_{22}) = 0 \; for \; \epsilon_{22} < 0 \tag{2.9}$$

where t_1, t_2, and t_3 are constants.

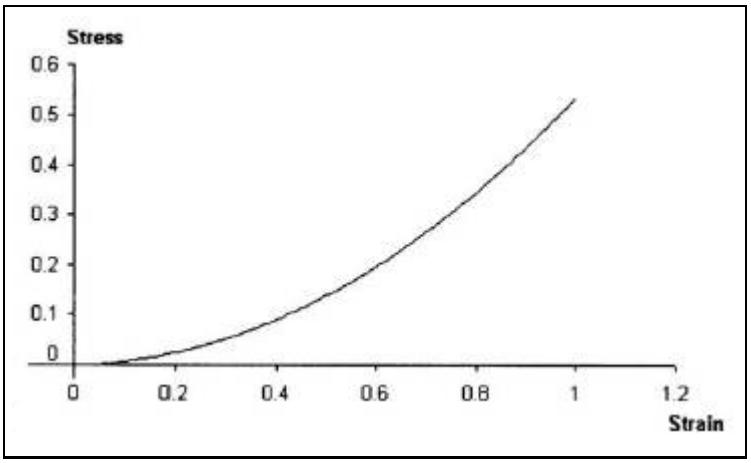

Figure 2.3 Mechanical properties representing the titin filaments which is dominating the passive resistance in the myofiber element valid only in the local fiber direction.

2.1.3 Aponeurosis Element

In order to represent the aponeuroses, a standard 3D, 8-node element HYPER58, from the element library of ANSYS 9.0 is used. This element has a hyperelastic mechanical formulation for which the strain energy density function is defined using the two parameter Mooney-Rivlin material law:

$$W = a_{10}(\overline{I}_1 - 3) + a_{01}(\overline{I}_2 - 3) + \frac{K}{2}(\overline{I}_3 - 1)^2 \tag{2.10}$$

where, $\overline{I}_i$ are reduced invariants of right-Cauchy strain tensor for $i = 1, ..., 3$, a_{10} and a_{01} are Mooney-Rivlin material constants, $K = 2(a_{10} + a_{01})/(1 - 2\nu)$ is the bulk modulus and ν is the Poisson's ratio. The parameters used (Table 2.1) ensure sufficient stiffness for the aponeuroses for a representative role in force transmission and providing muscular integrity as in real muscle.

It is assumed that, at the initial muscle length in the passive state, the sarcomeres arranged in series within muscle fibers have identical lengths. Fiber direction strain within the fiber mesh allows assessment of the non-uniformity of lengths of sarcomeres: positive strain reflects lengthening and negative strain reflects shortening. Note that zero strain represents the undeformed state of sarcomeres (i.e., sarcomere length: 2.5) in the passive condition at initial muscle length. Model results obtained for muscle

length equaling 25.2 mm (referred to as low muscle length) as well as muscle optimum length were studied in particular.

2.1.4 Model of Isolated Intact EDL Muscle

EDL muscle of the rat was modeled. This muscle has a relatively simple geometry: it is a unipennate muscle with rather small pennation angles and minimal variation of the fiber direction within the muscle belly. The geometry of the model is defined as the contour of a longitudinal slice at the middle of the isolated rat EDL muscle belly. Three muscle elements in series and sixteen in parallel fill this slice. All aponeurosis elements have identical mechanical properties but using a variable thickness in the fiber-cross fiber plane, the increasing cross-sectional area of the aponeurosis toward the tendon is accounted for [27]. This model (referred to as non-paralyzed muscle) was studied after the entire muscle elements were activated maximally (for a description of the activation procedure see [Yucesoy et al. 2002]). Three fundamental muscle data are collected from the models: Length-force relationship, strain distribution and stress distribution. Length-force data usually can not be obtained for the entire active range of motion, therefore is extrapolated at low lengths. For this purpose curve fitting toolbox of Matlab was used. Note that the model generated and described by Yucesoy et al. (2002) has been validated with experimental data and a finer mesh is created in accordance with this model. The reliability of the new model is confirmed by comparison with previous mesh and presented in the results section.

2.1.5 Models of EDL Muscle Representing the Principles of the Mechanical Effects of Botulinum Toxin

Clinically, Botulinum toxin is administered at multiple locations using smallest possible effective dose [28] in order to avoid antibody production by the immune system. Consequently, the target muscle is typically paralyzed partially [29, 30].

The effects of Botulinum toxin were modeled by activating only selected muscle elements within the muscle, whereas the remainder of the elements was left non-activated. Three separate cases studied allowed studying the principles of the mechanism of acute effects of Botulinum toxin on muscular mechanics:

1. Proximal half (fascicles 1-8) paralyzed (PHP)
2. Middle half (fascicles 5-12) paralyzed (MHP)
3. Distal half (fascicles 9-16) paralyzed (DHP)

Note that (1) for all Botulinum toxin cases the numbers of non-activated muscle fascicles were equal i.e., muscle volume representing the effects of Botulinum toxin was approximately the same. (2) Muscle volume including non-paralyzed muscle elements exclusively was referred to as the "mechanically operational muscle portion".

2.1.6 Solution Procedure

The analysis type used in ANSYS was static and large strain effects were included. A force based convergence criterion was used with a tolerance of 0.5%. Subsequent to maximal activation of the whole muscle (for the non-paralyzed muscle case) or mechanically operational muscle portions (for the cases modeling in principle the effects of Botulinum toxin), muscle length was altered by changing the position of muscle distal tendon.

Table 2.1
Values and definitions of the model constants

	Value	Unit	Definitions
k	0.05	N/mm2	Initial passive stiffness (Eq 2.4)
a_{11}	8.0	-	Passive cross-fiber direction stiffness ($a_{11} = a_{33}$
a_{22}	6.0	-	Passive fiber direction stiffness (Eq 2.4)
a_{12}	6.0	-	Passive fiber-cross-fiber shear stiffness, ($a_{12} = a_{23} = a_{31}(Eq2.4)$
S_s	10.0	N/mm2	Weight factor in the penalty function for the solid volume (Eq. 2.5)
S_f	10.0	N/mm2	Weight factor in the penalty function for the fluid volume (Eq. 2.5)
b_1	30.0	-	Coefficient for the stress-strain relation of the contractile elements (Eq 2.6)
b_2	-6.0	-	Coefficient for the stress-strain relation of the contractile elements (Eq 2.6)
b_3	1	-	Coefficient for the stress-strain relation of the contractile elements (Eq 2.6)
t_1	0.522	-	Coefficient for the stress-strain relation of the intracellular passive elements (Eq 2.7)
t_2	0.019	-	Coefficient for the stress-strain relation of the intracellular passive elements (Eq 2.7)
t_3	-0.002	-	Coefficient for the stress-strain relation of the intracellular passive elements (Eq 2.7)
a_{10}	7.9	N/mm2	Mooney-Rivlin material constant for aponeurosis elements (Eq. 2.8)
a_{01}	7.9	N/mm2	Mooney-Rivlin material constant for aponeurosis elements (Eq. 2.8)
ν	0.3	-	Poisson's ratio for aponeurosis elements (Eq. 2.8)

3. RESULTS

3.1 LFMM Model with Increased Number of Elements

The original muscle model developed by Yucesoy et al. (2002) is composed of three muscle elements in series and six in parallel. In this arrangement, the three series elements represent a muscle fiber bundle. This arrangement was shown to be sufficient and compatible to the experimental results. However in order to understand the mechanical effects of Botulinum toxin treatment, larger parallel element number was essential. Therefore as an initial step, generation of a finer mesh was necessary.

After Botulinum toxin injection, various fascicles are paralyzed within the muscle. In the model, the elements in series representing the fascicles would remain passive altogether to simulate this effect. Therefore increasing the number of parallel elements has been a priority. Two finer meshes, (1) 4 in series 12 in parallel (4x12) arrangement and (2) 3 in series 16 in parallel (3x16) arrangement, have been created and validated by comparing model results with initial 3 in series 6 in parallel (3x6) arrangement. Two main parameters were taken into account for comparisons: i) length-force characteristics, ii) strain distributions.

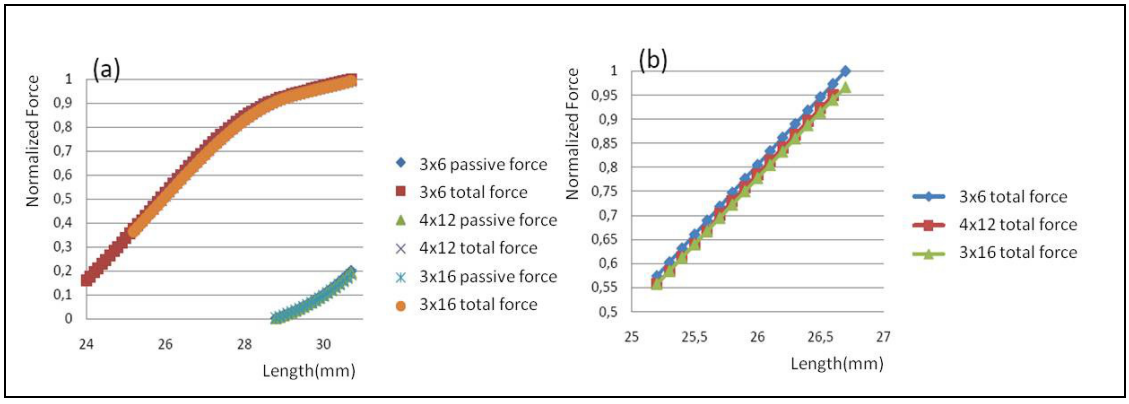

Figure 3.1 (a) Normalized total length-force curves for fully activated three meshes (b) Normalized length-force curves at low lengths. Total force gives the sum of active and passive forces

Comparison of the length-force characteristics obtained using the new meshes

with that of the original 3x6 arrangement Figure 3.1 shows that (i) the total force differs only by 0.8% at maximum and (ii) the passive forces differs only by 4.5% for 4x12 arrangement and 7.5% for 3x16 arrangement. These minor differences showed that both meshes may be used for Botulinum toxin study. Note that having more elements in the same volume also leads to finer resolution of the strain, stress distributions. This effect may be seen better with strain distributions (Figure 3.2).

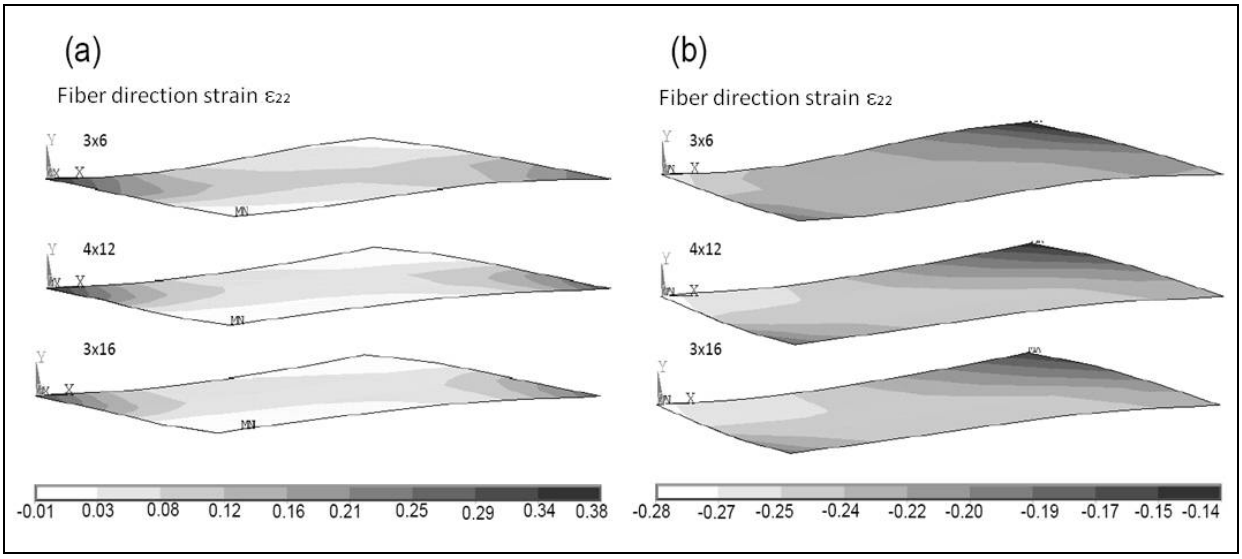

Figure 3.2 Fiber direction strain distributions at (a) high length (30.7 mm) and (b) low length (26.7 mm). The strain values give percentage length changes. Positive values indicate lenghtening whereas negative values indicate shortening

At high length, fiber direction strains range between -0.01 and 0.36 for original 3x6 arrangement. This range is found to be from -0.01 to 0.38 for 4x12 arrangement and from -0.01 to 0.32 for 3x16 arrangement. At low length the values are from -0.28 to -139, from -0.28 to -0.144 and from -0.28 to -0.154 for 3x6, 4x12 and 3x16 arrangements respectively. The fiber direction strain value differences are in accordance to those found in length-force data.

After the analysis given above, it is concluded that both arrangements are sufficient compared to original arrangement and give higher resolution in addition. Higher parallel element number would make it possible to simulate the Botulinum toxin paralyzation patterns more in detail. Therefore for the future studies, the 3x16 arrangement

which has highest parallel element number was preferred.

3.2 Effects of Botulinum Treatment on Muscle Length-Force Characteristics

For the fully isolated muscle, Figure 3.3 shows muscle active length-force characteristics for modeled non-paralyzed EDL and Botulinum toxin cases.

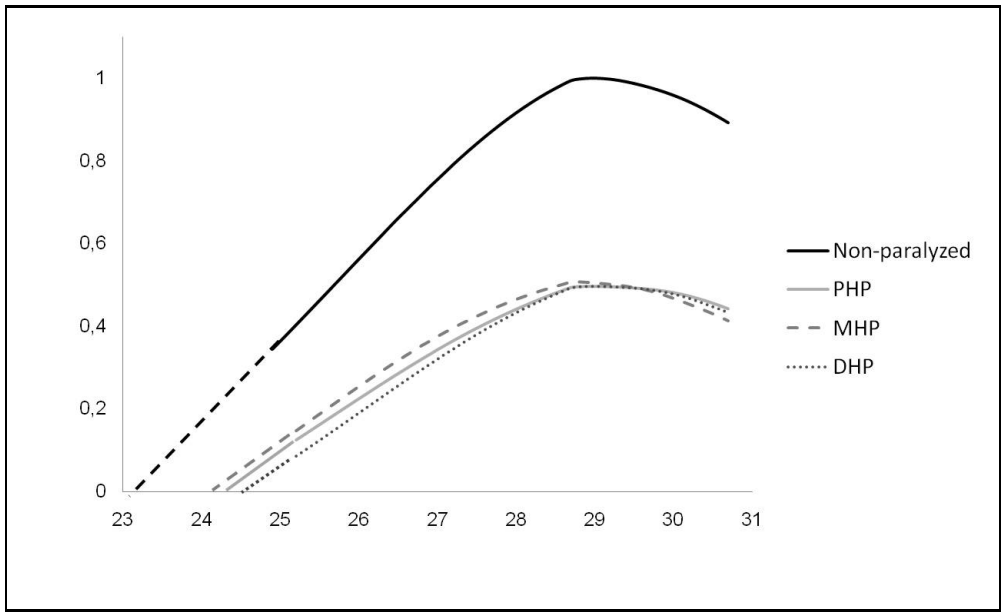

Figure 3.3 Active Length-Force Curves for Non-paralyzed case and Botulinum toxin cases. The force values are normalized by maximum of non-paralyzed case

A remarkable result is that substantial force decreases at all lengths are shown for Botulinum toxin cases: e.g., at muscle optimum length, force production of cases PHP, MHP and DHP were 49.7%, 50.7% and 49.6% of that of the non-paralyzed muscle, respectively. However, note that the differences between different Botulinum toxin cases were not considerable at higher muscle lengths. In contrast, at lower lengths, the difference in muscle active force among Botulinum toxin cases is more pronounced. At 25.2 mm (3.5 mm below muscle optimum length), muscle active forces dropped to 30.7%, 36.5% and 21.4% of that of the non-paralyzed muscle for cases PHP, MHP and DHP, respectively.

Botulinum toxin cases did not show appreciable shifts in muscle optimum length to a higher length (maximum shift equals about 1%). However, muscle active slack length did shift to higher lengths, decreasing the range of active force exertion by approximately 18.6%, 17.0% and 23.7% for cases PHP, MHP and DHP, respectively.

It is concluded that optimum force drop in accordance with the volume paralyzed and paralyzation of distal fiber population with Botulinum toxin leads to higher force drop at low lengths but also means lower range of active force exertion.

3.3 Effects of Location of Botulinum toxin Treatment on Lengths of Sarcomeres

Figure 3.4 shows distributions of fiber direction strains for non-paralyzed muscle and Botulinum toxin cases for optimum length. Note that in non-paralyzed muscle at optimum length, all sarcomeres are at the ascending limb of their length-force curves after activation (fiber direction strain ranges between -0.145 and -0.059). In contrast, for the Botulinum toxin cases due to paralyzation, sarcomeres located in the passive parts the muscles attain longer lengths (even positive strains as much as 0.02 were seen). This has effects for the entire muscle as well: maximum shortening equals to 14.5% in non-paralyzed muscle whereas for Botulinum toxin cases this is considerably less: maximum shortening equals 9% and 11% for cases PHP and DHP, respectively.

Remarkably, paralyzed muscle portions show increased parallel sarcomere length distributions at PHP an DHP: strain values range from -0.71 to 0.02. However, mechanically operational muscle portions have no notable increase in parallel distributions: between -0.108 and -0.71 for PHP and DHP.

Figure 3.5 shows the fiber direction strain distributions at low length. Similar to optimum length, Botulinum toxin cases show less sarcomere shortening however, this is not as consistent and pronounced: minimum shortening values are 0.1 for PHP

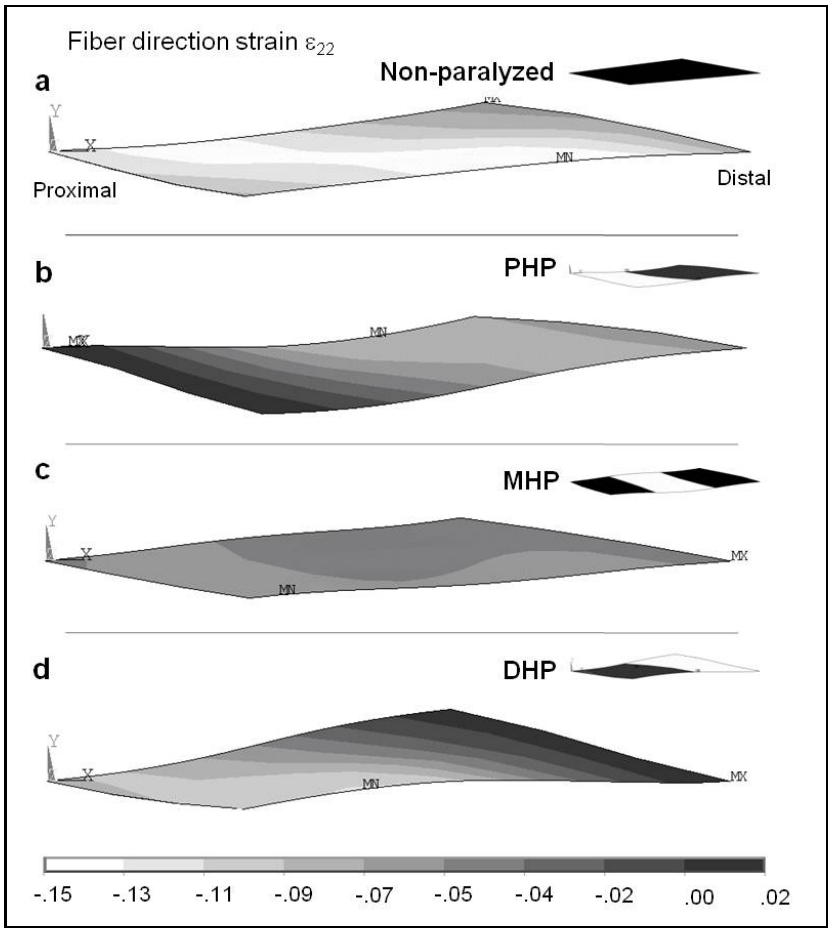

Figure 3.4 Fiber direction strain distributions at optimum length (28.7 mm muscle length) of (a) non-paraylzed muscle (b) proksimal half paralyzed muscle (c) middle half paralyzed muscle (d) distal half paralyzed muscle. Figures at the right top corners of each case shows the active parts in black and paralyzed parts in white. Color legend below the figures applies to all cases and gives percentage length changes. Negative values indicate shortening whereas positive values indicate lengthening.

and DHP whereas the value is 0.2 for non-paralyzed muscle model. Mechanically operational muscle portions show substantial sarcomere length heterogeneity e.g. DHP ranges from -0.39 to -0.13 whereas the non paralyzed muscle model ranges between -0.36 and -0.23.

The differences in fiber direction stains among different cases are indicated to originate from the interaction between paralyzed and mechanically operational muscle portions. Therefore, effects of Botulinum toxin treatment on sarcomere length distributions are studied in further detail by distinguishing the two portions and comparing them with their counterparts non-paralyzed muscle model.

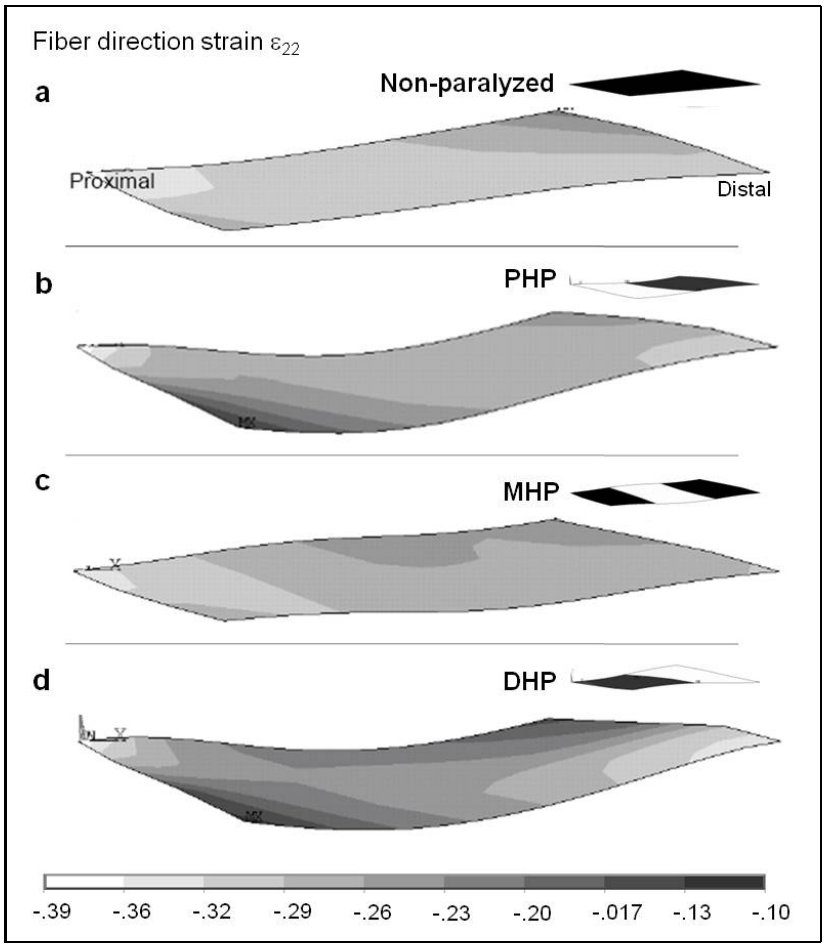

Figure 3.5 Fiber direction strain distributions at low length (25.2 mm muscle length) of (a) non-paraylzed muscle (b) proksimal half paralyzed muscle (c) middle half paralyzed muscle (d) distal half paralyzed muscle. Figures at the right top corners of each case shows the active parts in black and paralyzed parts in white

Figure 3.6 does clearly show the less pronounced sarcomere shortening in the mechanically operational muscle portions of the Botulinum toxin cases. This effect substantiates towards the interface between paralyzed and mechanically operational muscle portions: e.g. at node 9 the strain values for PHP and DHP are -0.07 and -0.05 respectively whereas for non-paralyzed muscle this value is -0.011 at I. Note that, case MHP has two of such interfaces and hence the lowest sarcomere shortening after activation: e.g. the strain value of node 5 at I is -0.05 whereas its counterpart in non-paralyzed muscle shortens as much as -0.13 percent.

This effect of less pronounced sarcomere shortening in the mechanically operational muscle portions of the Botulinum toxin cases is valid also for low muscle length

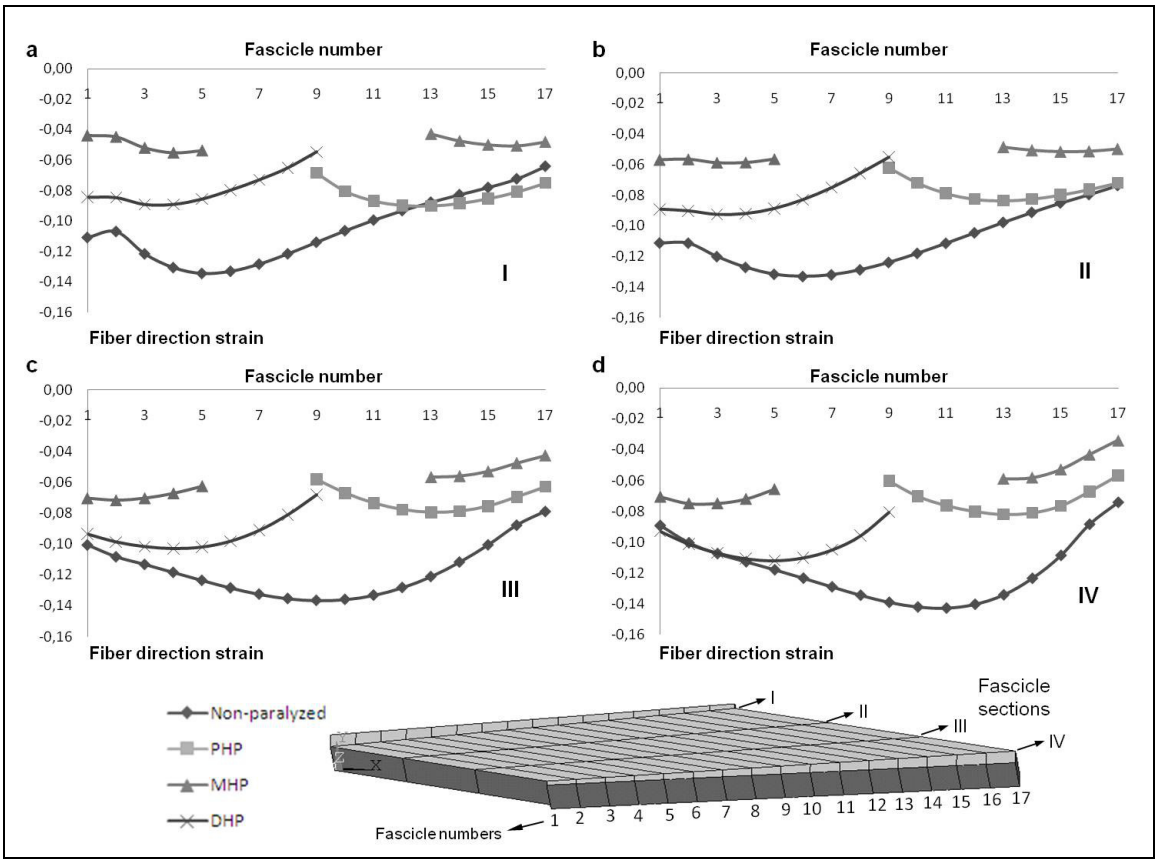

Figure 3.6 Nodal fiber direction strain values at optimum length for mechanically operational muscle portions

(Figure 3.7): the difference in shortening reaches to 16% of that of the non-paralyzed muscle for case PHP.

In spite of the distinct differences in sarcomere shortening, coefficient of variation values calculated for the mean strain values (Figure 3.8) does not show a sizable difference in fiber strain heterogeneity: readily not so high coefficient of variation for the non-paralyzed muscle did not change considerably in Botulinum toxin cases. It was found to be 1.97 for non paralyzed muscle and drops to 0.74 at most for MHP case. The values are found to be 0.82 for PHP and 1.24 for DHP.

It is concluded that number of interfaces between paralyzed and non-paralyzed portions directly affects the strain distributions.

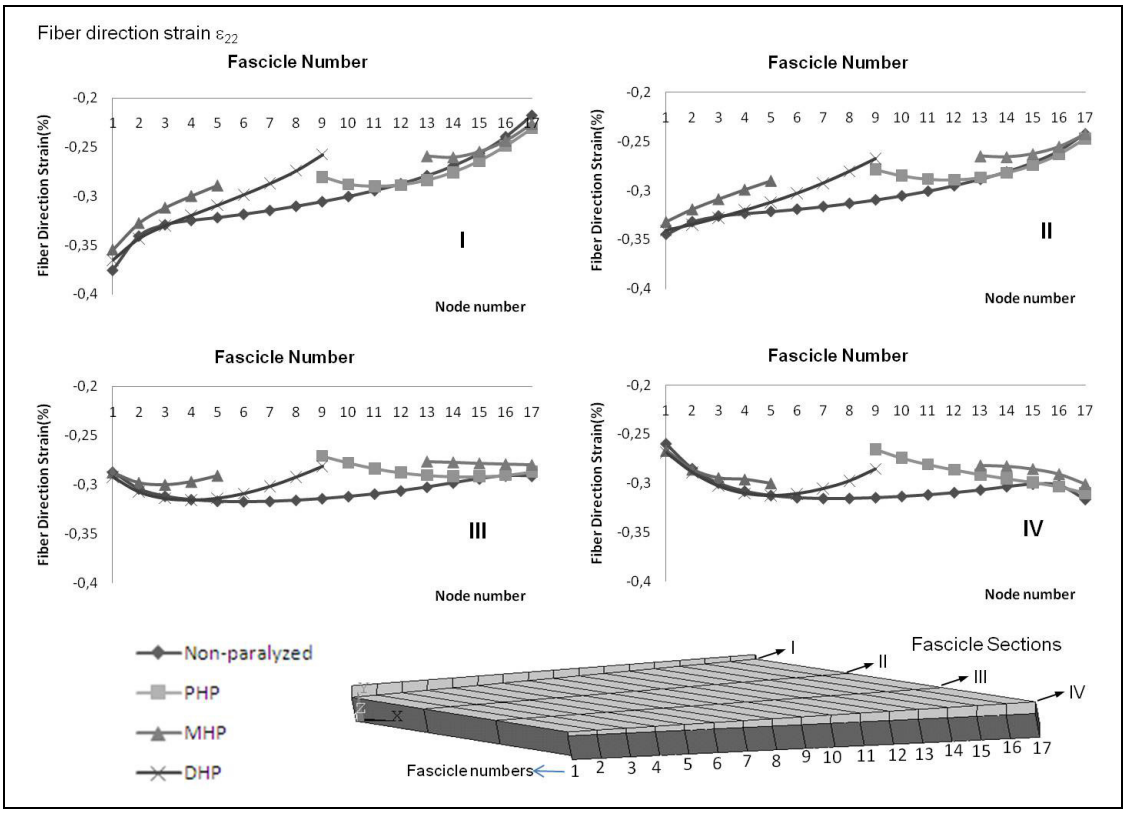

Figure 3.7 Nodal fiber direction strain values at short length for mechanically operational muscle portions

3.4 Effects of Location of Botulinum toxin Treatment on Force Production

Less pronounced sarcomere shortening found in Botulinum toxin cases for muscle lengths equal to and lower than muscle optimum length suggests occurrence of a greater capacity of force generation within the mechanically operational muscle portions. This is confirmed by examining mean fiber stresses (Figures 9, 10).

The area under mean stress curve is taken as an index of capacity of force exertion. At muscle optimum length (Figure 3.9) this area for PHP, MHP and DHP respectively equals to 50%, 53% and 47% that of non-paralyzed muscle showing that the overall force exertion capacity is reduced in agreement with the force drops.

On the other hand, the mechanically operational muscle portions of the Bo-

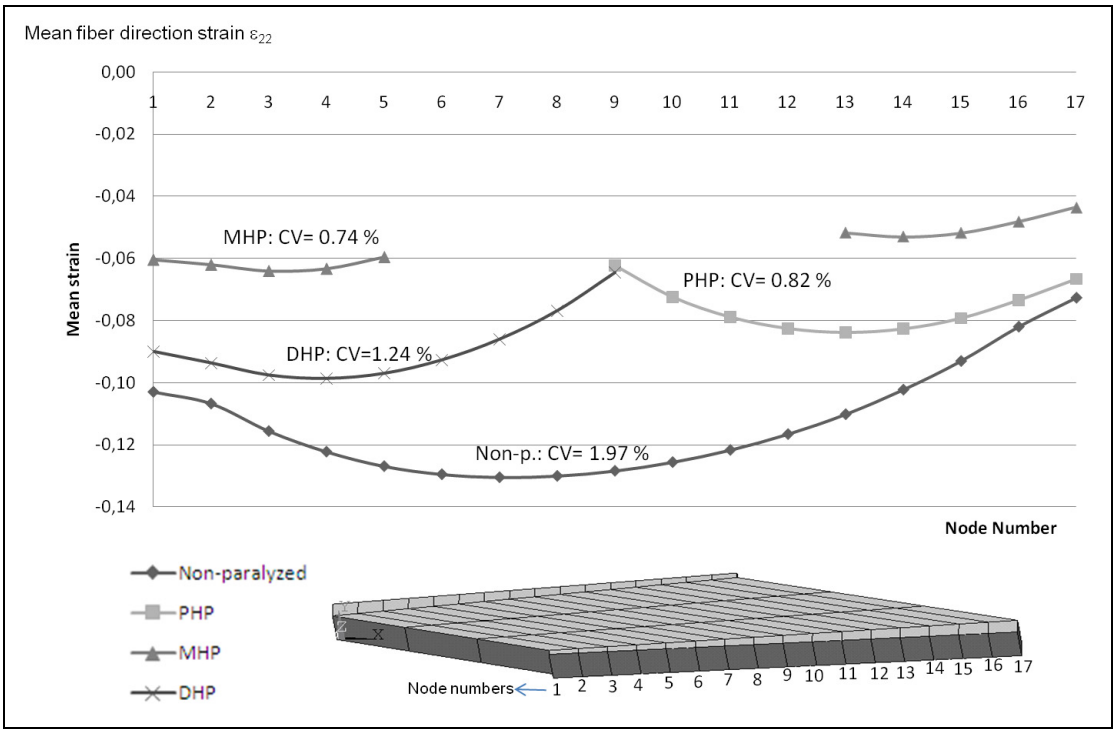

Figure 3.8 Mean nodal strain values of mechanically operational muscle portions at optimum length with coefficient of variation values (CV)

tulinum toxin cases are capable of producing a higher force (by 3%, 9% and 5% for PHP, MHP and DHP, respectively) than the same portion of the non-paralyzed muscle.

At low muscle length, the area under mean fiber stress curve for cases PHP, MHP and DHP respectively equals 53%, 55% and 30% that of non-paralyzed muscle. Also, mechanically operational muscle portion of PHP, MHP and DHP is capable of producing a higher force (by 11% 12% and 7%, respectively) compared to the same portion of the non-paralyzed muscle.

It is concluded that mechanically operational portions of Botulinum toxin cases have higher capacities of force production compared to their counterparts in non-paralyzed case.

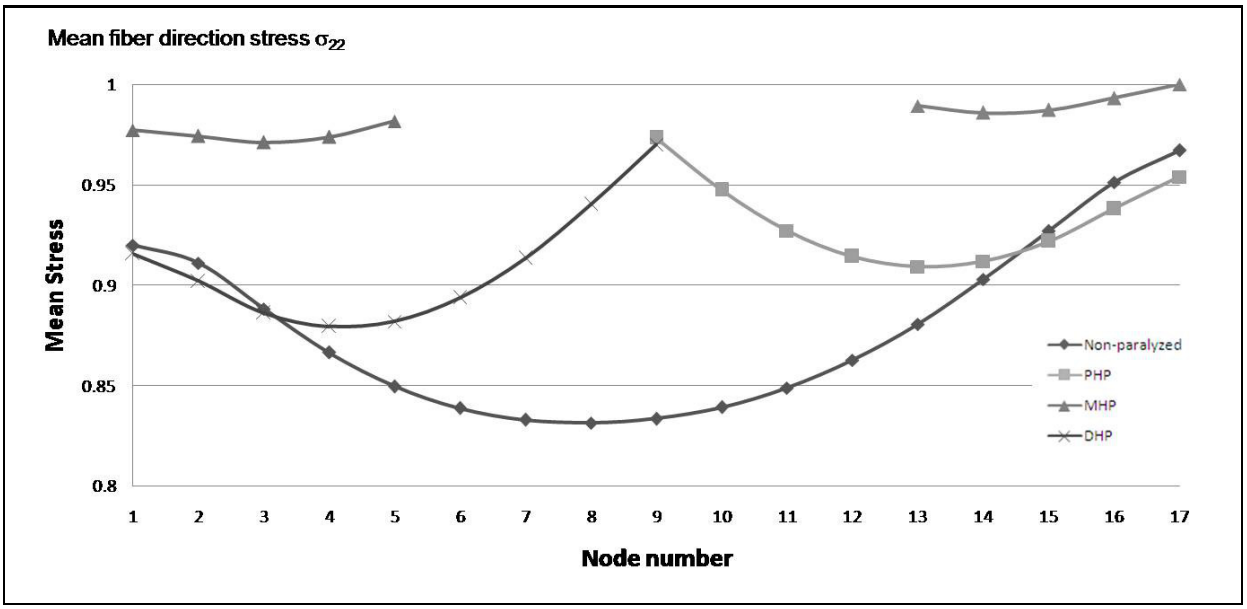

Figure 3.9 Mean fiber direction nodal stress values at optimum length for mechanically operational muscle portions. Stress values are normalized in the model such that zero strain corresponds to 1.00 stress value

3.5 Myofascial Force Transmission

Since the model is fully isolated, the effect can be only due to intra-muscular connections, i.e. only intra-muscular myofascial force transmission may exist. Still, less sarcomere shortening in Botulinum toxin cases in the mechanically operational muscle portions is caused by myofascial force transmission: if muscle fibers were to function independently, the ones in Botulinum toxin muscle would have been shortened identically to those located in the non-paralyzed muscle. However, their shortening is limited due to their interaction with the paralyzed muscle fibers which remained at higher lengths after contraction. This effect is more pronounced in MHP case, which has two interfaces between mechanically operational parts and paralyzed parts.

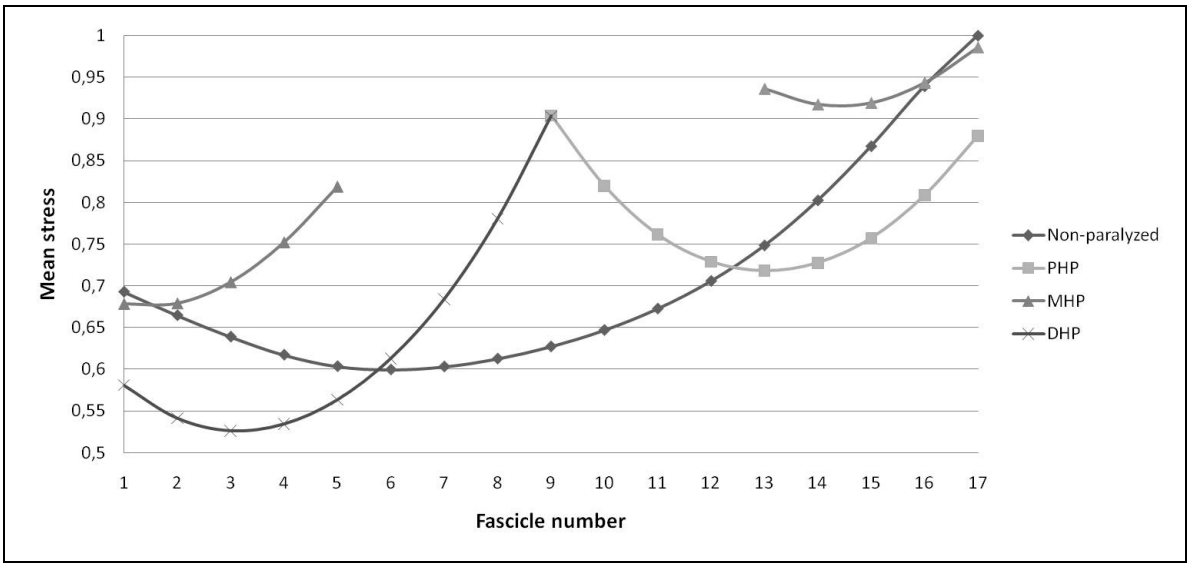

Figure 3.10 Mean fiber direction nodal stress values at low length for mechanically operational muscle portions. Stress values are normalized in the model such that zero strain corresponds to 1.00 stress value

4. DISCUSSION

4.1 Fundamental Effects of Botulinum Toxin Treatment

Studies conducted both on animals and humans showed that Botulinum toxin leads to formation of paralyzed zones within the target muscles and causes reduction of muscular force[22, 31, 32]. Because of this property Botulinum toxin has been widely used for treatment of disorders causing abnormal muscle activity such as cerebral palsy [22, 33]. Consequently, it is aimed at controlling the limitation in the joint range of motion by disrupting the imbalance of joint moment, in favor of the weaker antagonistic muscles.

This study clearly showed that in spite of a major force drop, active range of joint motion decrease. It is known that spastic muscle fascicles operate at lower lengths compared to healthy muscle, limiting active range of motion may even below optimum length [34]. Functionality of Botulinum toxin treatment might be the result of active range motion being limited to higher lengths. But an important model result showed that this effect is not necessarily achieved by a shift in optimum length.

4.2 Myofascial Force Transmission and its Implications

Despite its wide use, the mechanical mechanism of Botulinum toxin has not been understood clearly. Direct approaches on muscular effects owe it to the restrained point of view on muscular mechanics by the classical approach [35]. In classical view of force transmission, muscle force generated by the myofibers is considered entirely to be transmitted to the tendon and from there onto the bony skeleton to cause movement. In many cases this path of force transmission is implicitly assumed to be the exclusive channel [4]. However the role played by the continuous system of connective tissues in force transmission, i.e. myofascial force transmission, has been made evident later [4].

Accordingly, treatment approaches derived from classical view utilize a single sarcomere length value, and not a possible sarcomere length heterogeneity [36].

In contrast, the present study showed that similar to previous studies [16, 18, 15], Botulinum toxin increases sarcomere length heterogeneity in the fiber. In isolated muscle, the mechanical mechanism of Botulinum toxin arises from i) absence of shortening at the paralyzed muscle portions, ii) less shortening of mechanically operational portions compared to their counterparts in non-paralyzed muscle. The sarcomere length difference becomes more pronounced at low lengths between paralyzed and non-paralyzed portions. This in return leads to an increased heterogeneity of sarcomere lengths. Nevertheless, such heterogeneity is not immediately functional mechanicaly since paralyzed parts do not contribute to muscle force directly. Even so, paralyzed parts effect mechanically operational portions, causing less shortening, and therefore change the muscle mechanics. In Botulinum toxin cases, the whole muscle shows parallel sarcomere length distribution (except for MHP), originating from the paralyzed muscle portions. Although it would have no direct effect on (optimal) muscle force, it may have implications for adaptation [37].

Less shortening of active parts of Botulinum toxin cases seen in Figures 3.7 and 3.8 requires an interaction between paralyzed and active parts of the muscle. This interaction is a direct consequence of intra-muscular myofascial force transmission. Such limited connections leading to major effects is an indicator of why myofascial force transmission should be the major determinant of the mechanical mechanism of the effects of Botulinum toxin. A muscle in-vivo, having all the connections intact, would be affected not only by intra-muscular connections but also by epi-muscular connections. Recent studies showed that epimuscular myofascial force transmission is capable of causing major effects within the entire lower leg of the rat [38] and therefore change the length-force characteristics of a muscle. Moreover, sarcomere length distributions are altered greatly [16]. Therefore effects of paralyzation found in this study may be enhanced and further alteration in length-force characteristics such as a shift in optimum force and different sarcomere length distributions may be found with every level connections.Knowing the intramuscular dynamics with this study will

make it possible to identify and differentiate the effects of these connection types.

The change in the sarcomere length distributions may also have adaptive effects. Our recent studies hint that local effects such as extreme deformations adaptation may occur. This possibility can also be addressed in further studies.

4.3 Limitations of the Study

A study by Trotter et al. (1992) [7] proved the myofascial force transmission with the existence of non-spanning fibers. Non-spanning fibers do not span the whole muscle from one aponeurosis to another but are terminated intrafascularly. Therefore in order for such a fiber to transmit its force, intramuscular myofascial force transmission is neccessary. In this study, the paralyzation due to Botulinum toxin is modeled by leaving desired parts inactivated completely. In the end, with fascicles spanning the whole length between two aponeuroses, we have a whole block of inactive fascicles. Partial activation as the effect of Botulinum toxin ceases may also be possible. Nevertheless, internal mechanical mechanism is expected to remain similar since less shortening of the partial paralyzed parts would still affect the mechanically operational muscle portions.

Another limitation is, the mechanical properties of the modeled EDL muscle and its intramuscular connections represent those of healthy muscle. Some differences were suggested to exist between spastic and healthy muscle mechanics [39]. The spastic muscles are reported to be stiffer than healthy muscle both in muscular and connective level [40]. These differences might have important effects such as even lesser shortening of the fibers in mechanically operational muscle portions since a stiffer collagen matrix would work against the fiber contraction. Therefore the basic principles of mechanical effects of the treatment would remain the same or even be more pronounced.

4.4 Prospective Studies

In this study on isolated muscle myofascial force transmission is limited to intramuscular myofascial force transmission. With more connections, additional effects will accumulate making it hard to differentiate the sources. But, our study showed that paralyzed muscle portions limit the shortening or lengthening of active parts. With the help of this fact differentiating the sources will be possible. Further studies should include increased connections to fully simulate in-vivo situation. Also paralyzation patterns based on experimental data would lead to knowledge on actual situation.

REFERENCES

1. A. Faller, M. S., *The Human Body An Introduction to Structure and Function*, Stuttgart, New York: Thieme, 13th ed., 1999.

2. Saladin, K. S., *Saladin: Anatomy and Physiology: The Unity of Form and Function*, The McGraw-Hill Companies, 2003.

3. Valerie C. Scanlon, T. S., *Essentials of Anatomy and Physiology*, Philadelphia: F. A. Davis Company, 2007.

4. Huijing, P. A., "Muscle as a collegen fiber reinforced composite: a review of force transmission in muscle and whole limb," *Journal of Biomechanics*, Vol. 32, pp. 329–345, 1999.

5. Tidball, J. G., "Myotendinous junction injury in relation to junction structure and molecular composition," *Exerc Sport Sci Rev*, Vol. 19, pp. 419–445, 1991.

6. Trotter, J., "Functional morphology of force transmission in skeletal muscle. a brief review," *Acta Anat*, Vol. 146, pp. 205–222, 1993.

7. Trotter, J. A., and P. P. Purslow, "Functional morphology of the endomysium in series fibered muscles," *Journal of Morphology*, Vol. 212, pp. 109–122, 1992.

8. Hijikata T, Wakisaka H, N. S., "Functional combination of tapering profiles and overlapping arrangements in nonspanning skeletal muscle fibers terminating intrafascicularly," *Anat Rec*, Vol. 236, pp. 602–610, 1993.

9. Tidball JG, D. T., "Myotendinous junctions of tonic muscle cells: Structure and loading.," *Cell Tissue Res*, Vol. 245, pp. 315–322, 1986.

10. Tidball, J. G., "The geometry of actin filament-membrane associations can modify adhesive strength of the myotendinous junction," *Cell Motil*, Vol. 3, pp. 439–447, 1983.

11. Rack P., W. D., "Elastic properties of the cat soleus tendon and their functional importance," *J. Physiol*, Vol. 347, pp. 479–495, 1984.

12. Street, S. F., "Lateral transmission of tension in frog myofibers: a myofibrillar network and transverse cytoskeletal connections are possible transmitters," *Journal of Cellular Physiology*, Vol. 114, pp. 146–364, 1983.

13. Ramsey R. W., S. S. F., "The isometric length-tension diagram of isolated skeletal muscle fibers of the frog," *Journal of Cellular and Comparative Physiology*, Vol. 15, pp. 11–34, 1940.

14. Huijing P. A., G. Baan, G. R., "Non myo-tendinous force transmission in rat extensor digitorum longus," *Journal of Experimental biology*, Vol. 201, pp. 682–691, 1998.

15. C A Yücesoy, H. Koopman, G. B. H. G. P. A. H., "Pre-strained epimuscular connections cause muscular myofascial force transmission to affect properties of synergistic ehl and edl muscles of the rat," *Journal of Biomechanical Engineering*, Vol. 127, pp. 819–828, 2005.

16. Yücesoy, C. A., *Intra-, inter- and extra-muscular myofascial force transmission: A combined finite element modeling and experimental approach.* PhD thesis, University of Twente, Utrecht, The Netherlands, 2003.

17. H. Meijer, G. Baan, P. H., "Myofascial force transmission between antagonistic rat lower limb muscles: effects of single muscle or muscle group lengthening.," *Journal of Electromyography and Kinesiology*, Vol. 17, pp. 698–707, 2007.

18. H. Maas, G. Baan, P. H., "Intermuscular interaction via myofascial force transmission: effects of tibialis anterior and extensor hallucis longus length on force transmission from rat extensor digitorum longus muscle," *Journal of Biomechanics*, Vol. 34, pp. 927–940, 2001.

19. N. Mahant, P. D. Clouston, I. T. L., "The current use of botulinum toxin," *Journal of Clinical Neuroscience*, Vol. 7, no. 5, pp. 389–394, 2000.

20. Klein, A. W., "Complications, adverse reactions, and insights with the use of botulinum toxin," *Dermatol Surg*, Vol. 29, pp. 549–556, 2003.

21. H. Kerr Graham, K. R. A., "Recommendations for the use of botulinum toxin type a in the management of cerebral palsy," *Gait and Posture*, Vol. 11, pp. 67–79, 2000.

22. Parratte, B., T. L. V. F. D. M., "Intramuscular distribution of nerves in the human triceps surae muscle: anatomical bases for treatment of spastic drop foot with botulinum toxin," *Surg Radiol*, Vol. 24, pp. 91–96, 2002.

23. Borodic G., R. Ferrante, L. P. K. S., "Histologic assessment of dose-related diffusion and muscle fiber response after therapeutic botulinum a toxin injections," *Mov Disord*, Vol. 9, pp. 31–39, 1994.

24. Huyghe, J. M., D. H. van Campen, T. Arts, and R. M. Heethaar, "A two-phase finite element model of the diastolic left ventricle," *Journal of Biomechanics*, Vol. 24, pp. 527–538, 1991.

25. Zuurbier, C. J., J. W. Heslinga, M. B. L. de Groot, and W. J. V. der Laarse, "Mean sarcomere length-force relationship of rat muscle fiber bundles," *Journal of Biomechanics*, Vol. 28, pp. 83–87, 1995.

26. Trombitas, K., J. P. Jin, and H. Granzier, "The mechanically active domain of titin in cardiac muscle," *Circulation Research*, Vol. 77, pp. 856–861, 1995.

27. C J Zuurbier, A. J. Everard, P. V. d. W. P. A. H., "Length-force characteristics of the aponeurosis in the passive and active muscle condition and in the isolated condition," *Journal of Biomechanics*, Vol. 27, pp. 445–453, 1994.

28. Brin, M., "Botulinum toxin: Chemistry, pharmacology, toxicity, and immunology," *Muscle Nerve*, Vol. 20, pp. 146–168, 1997.

29. Metezeau P, D. M., "Botulinum toxin type a: kinetics of calcium dependent paralysis of the neuromuscular junction and antagonism by drugs and animal toxins," *Toxicon*, Vol. 20, no. 3, pp. 649–54, 1982.

30. C. M. Shaari, I. S., "Quantifying how location and dose of botulinum toxin injections affect muscle paralysis," *Muscle Nerve*, Vol. 16, pp. 964–969, 1993.

31. Spencer R. F., McNeer, K. W., "Botulinum toxin paralysis of adult monkey extraocular muscle. structural alterations in orbital, singly innervated muscle fibers," *Arch Ophthalmol*, Vol. 105, pp. 1703–1711, 1987.

32. Harris C., K. Alderson, J. N. J. H., "Histologic features of human orbicularis oculi treated with botulinum a toxin," *Arch Ophthalmol*, Vol. 109, pp. 393–395, 1991.

33. Fock J., M. Galea, B. S. B. R. M. C., "Functional outcome following botulinum toxin a injection to reduce spastic equinus in adults with traumatic brain injury," *Brain Inj*, Vol. 18, pp. 57–63, 2004.

34. Moreau NG, Teefey SA, D. D., "In vivo muscle architecture and size of the rectus femoris and vastus lateralis in children and adolescents with cerebral palsy," *Dev Med Child Neurol*, Vol. 51, no. 10, pp. 800–806, 2009.

35. Berthier C., S. B., "Supramolecular oraganization of the subsarcolemmal cytoskeleton of adult skeletal muscle fibers. a review," *Biology of the Cell*, Vol. 89, pp. 413–434, 1997.

36. Lieber R. L., J. F., "Intraoperative measurement and biomechanical modeling of the flexor carpi ulnaris-to-extensor carpi radialis longus tendon transfer," *Journal of Biomechanical Engineering*, Vol. 119, no. 4, pp. 386–391, 1997.

37. Huijing P A, R. T. J., "Adaptation of muscle size and myofascial force transmission: a review and some new experimental results," *Scand J Med Sci Sports*, Vol. 15, pp. 349–380, 2005.

38. Yücesoy C A, Guus Baan, P. A. H., "Epimuscular myofascial force transmission occurs in the rat between the deep flexor muscles and their antagonistic muscles," *Journal of Electromyography and Kinesiology*, Vol. 20, pp. 118–126, 2010.

39. Booth CM, Cortina-Borja MJ, T. T., "Collagen accumulation in muscles of children with cerebral palsy and correlation with severity of spasticity," *Dev Med Child Neurol*, Vol. 43, no. 5, 2001.

40. Tardieu G, Tardieu C, C.-J. P. B. M., "Effects of muscle length on an increased stretch reflex in children with cerebral palsy," *J Neurol Neurosurg Psychiatry*, Vol. 45, pp. 348–52, 1982.